

NONLINEAR EXTENT OF POPULATION PRESSURE ON VEGETATION COVER CAUSING TOPSOIL FERTILITY LOSS: A MATHEMATICAL MODEL

¹*Sarki D.S.*, ²*Pam B.D.*, ³*Bwirdimma D.G* and ⁴*Sarki B.D.*

^{1,3}Department of Mathematics, Federal College of Education Pankshin, Plateau State, Nigeria

²Department of Computer Sciences, Federal College of Education Pankshin, Plateau State, Nigeria

⁴Department of Science and Technology, Faculty of Education, University of Jos, Plateau State, Nigeria

Abstract

A nonlinear mathematical model is proposed analysed to study the extent of increasing human population pressure on vegetation cover and the consequential fallout on the fertility of fertile topsoil. The model is analysed using the stability theory of differential equations and numerical simulation. It was shown, among other findings, that allowing population pressure to continue to increasing has the consequential effect of decreasing the density of vegetation cover thereby reducing soil nutrient uptake due to reducing vegetation density. Numerical simulation of the model validated analytical results.

1. Introduction

The livelihood of a substantial number of the world's population depend on forestry resources [1]. These resources include, but not limited to food, fresh water, clothing, herbs, shelter [1]. These benefits are under enormous threat in recent times [1, 2]. The types of vegetation and how well they can grow on particular soil types are basically influenced by soil physical – properties: soil texture, structure, porosity, soil density, drainage and surface hydrology. These properties play a major role on soil erodibility [3]. Soil microorganisms are vital for the functioning and long-term sustainability of the ecosystem. The scantiness or lack of vegetation cover exacerbates wind erosion [3]. Forest soils with a carpet of decomposing leaves absorb rainwater like a sponge, holding the water for gradual release to streams throughout the year [1]. Tillage and cropping practices, known to lower soil organic matter and deplete soil structure, among others, are important erosion causal factors [4]. Soil is the epicentre of a very complex elemental interaction. its loss has been estimated as a function of the extent of these interacting components, for instance, precipitation pattern, topographical setting, physical transporting processes, economic diversification, social integration, legislative and political interplay and conservation management strategies [4, 5]. Substantial information and insightful implications have been gotten from nonlinear mathematical studies on the extent of human pressure on forest resources [1, 5 – 10] and the various literatures they contain. However, to the best of our knowledge, there are no existing researches on the depletion of fertile topsoil incorporating mineral intake using nonlinear mathematical models. Thus, we intent to provide a nonlinear mathematical formulation that will study the extent of population pressure and mineral uptake aspects of soil degradation.

2. Model formulation

Let, in the region being considered and at any given time period t , $V(t)$ denotes the density of vegetation cover, $H(t)$ denotes population (human) density, $P(t)$ represents the density of deployable human pressure, $S(t)$ and $U(t)$ denote the mass of topsoil and concentration of soil mineral in absorbed phase. Pursuant to our research intention, we consider the following assumptions

1. Both the density of vegetation cover and population are governed by logistic type equations with L as the maximum sustainable population size under the given environmental and ecological constraints.
2. The mounting levels of population pressure at any given time is proportional to the corresponding population density at that time period
3. The mass of fertile topsoil has a constant natural growth rate
4. The concentration of absorbed soil mineral by vegetation is proportional to the density of vegetation and fertility of topsoil

From the forgoing, the system dynamics may be governed by the following system of nonlinear ordinary differential equations:

Correspondence Author: Sarki D.S., Email: dins@fcepanshin.edu.ng, Tel: +2348069739912

Transactions of the Nigerian Association of Mathematical Physics Volume 11, (January – June, 2020), 89–96

$$\begin{aligned}
 \frac{dV}{dt} &= \eta V - \eta_1 V^2 - \psi_1 HV - \psi_2 P \\
 \frac{dH}{dt} &= \gamma H \left(1 - \frac{H}{L}\right) + d\psi_1 HV, \\
 \frac{dP}{dt} &= \mu H - \rho_0 P - \rho_1 PS, \\
 \frac{dS}{dt} &= \Delta - \pi_0 S - \pi_1 SV - \pi_2 SP - \pi_3 SP^2, \\
 \frac{dU}{dt} &= \pi_1 SV - \phi_1 U - \phi_0 UV
 \end{aligned}
 \tag{1}$$

where $V(0) \geq 0, H(0) \geq 0, P(0) \geq 0, S(0) \geq 0, U(0) \geq 0$.

We propose that the density of vegetation cover at any given time period is affected by the fertility status of the soil as well as mounted level of human population pressure. Thus, the growth rate of vegetation cover, which grows intrinsically at a rate η , is decreased due to increasing human interferences. We assume that this decrease is proportional to the level of human intra specific competition at a rate η_1 , depletion rate due to population’s usage of vegetation for fuel, wood, shelter, roofing, food, fodder, herbs etc. at a constant rate ψ_1 , which simultaneously influences the growth of the population in proportion to the cumulative volume of vegetation resources used with proportionality constant d (such that $0 < \lambda < 0$). The parameter ψ_2 represents the depletion rate coefficient of vegetation cover due to the mounting population pressure like the irreversible clearing of land for agriculture, housing complexes and other infrastructural constructions. We therefore assume that this increase in population pressure is proportional, with constant μ , to the human population density and decreases following natural courses like ill health, incapacitation, death, etc. at rate ρ_0 , as well as due to deployable human effort on the soil at a rate ρ_1 . The second equation of the model system (1) has γ as its intrinsic population growth rate and L is the corresponding carrying capacity of the population in the absence of vegetation biomass. Further, the mass of fertile topsoil is assumed to grow naturally at a constant rate coefficient Δ and decreases naturally (for instance, due to gravitational force effect on topsoil) at a rate π_0 , due to vegetation cover on the soil surface at a rate π_1 , which simultaneously represent the soil concentration of nutrients absorbed by vegetation cover. π_2 and π_3 denote the depletion rate coefficients due to extreme human pressure on the soil surface assumed to be proportional to P and P^2 for agricultural and infrastructural expansions respectively. The constant ϕ_1 denotes the natural washout rate coefficient of absorbed nutrient concentration while ϕ_0 denote the depletion rate coefficient of absorbed nutrients concentration due to dying (harvesting, cutting down, burning etc.) of vegetation biomass.

3. Boundedness of the system

The boundedness of a system guarantees its validity. In this section, we establish the boundedness of the model system (1) through the following lemma.

Lemma. *The set $\Omega = \left\{ (V, H, P, S, U) : 0 \leq V \leq \frac{\eta}{\eta_1}; 0 \leq H \leq H_m; 0 \leq P \leq P_m; 0 \leq S + U \leq \frac{\Delta}{\pi_0 + \phi_1} \right\}$, is the region of attraction for the model system*

(1) and attracts all solutions initiating in the interior of the positive orthant, where $H_m = \frac{L}{\gamma\eta_1} (\gamma\eta_1 + \eta\lambda\psi_1)$ and $P_m = \frac{\mu L}{\gamma\rho_0\eta_1} (\gamma\eta_1 + \eta\lambda\psi_1)$.

Proof

It can be noted from the first equation of the model system that

$$\frac{dV}{dt} \leq \eta V - \eta_1 V^2,$$

which gives $0 \leq V(t) \leq \frac{\eta}{\eta_1}$.

We similarly observe from the second equation of the system that

$$H = \frac{L}{\gamma} (\gamma + \lambda\psi_1 V) \leq \frac{L}{\gamma\eta_1} (\gamma\eta_1 + \eta\lambda\psi_1) = H_m$$

Next, from the fourth equation of the model system (1), we can be noted that $\frac{dS}{dt} \leq \Delta - \pi_0 S \Rightarrow 0 \leq S(t) \leq \frac{\Delta}{\pi_0}$.

We can further note from the third and last equations of the model system (1), respectively, that

$$\frac{dP}{dt} \leq \mu H - \rho_0 P \Rightarrow 0 \leq P(t) \leq \frac{L}{\gamma\rho_0\eta_1} (\gamma\eta_1 + \eta\lambda\psi_1) = P_m.$$

and

$$\frac{dU}{dt} \leq \pi_1 SV - \phi_1 U \Rightarrow 0 \leq U(t) \leq \frac{\pi_1}{\phi_1} \frac{\eta\Delta}{\eta_1\pi_0}.$$

Hence, the prove of the Lemma.

4. Equilibrium analysis

The model system (1) has the following nonnegative equilibria

$$E_0(0,0,0,0,0), E_1(V_1,0,0,0,0), E_2(0,H_2,0,0,0), E_3(0,0,0,S_3,0), E_4(V_4,H_4,0,0,0), E_5(V_5,0,0,S_3,0), E_6(0,H_6,P_6,0,0), E_7(0,H_7,0,S_7,0), E_8(V_8,H_8,P_8,0,0), E_9(V_9,H_9,0,S_9,0), E_{10}(V_{10},H_{10},0,S_{10},U_{10}) \text{ and } E^*(V^*,H^*,P^*,S^*,U^*)$$

The existences of $E_0(0,0,0,0,0), E_1(V_1,0,0,0,0), E_2(0,H_2,0,0,0), E_3(0,0,0,S_3,0), E_5(V_5,0,0,S_3,0), E_6(0,H_6,P_6,0,0)$ and $E_7(0,H_7,0,S_7,0)$ are obvious without any condition. Those of $E_4(V_4,H_4,0,0,0), E_9(V_9,H_9,0,S_9,0)$ and $E_{10}(V_{10},H_{10},0,S_{10},U_{10})$ depends on the validity of $\eta > \psi$, that is, if the intrinsic growth rate of vegetation cover exceeds the corresponding basic utilisation need of man. Further, the existence of the equilibrium $E_8(V_8,H_8,P_8,0,0)$ is determined by the condition $\eta > \psi_1 L$ (that is if the intrinsic growth rate of green vegetation exceeds the cumulative expected vegetative need of man), in which case

$$V_8 = \frac{-a_1 + \sqrt{a_1^2 + 4\gamma\mu\lambda\rho_0\psi_1\psi_2L(\eta - \psi_1L)}}{2\mu\lambda\psi_1\psi_2L}, \text{ where } a_1 = \lambda\rho_0\psi_1^2L + \gamma(\rho_0\eta_1 + \mu\psi_2L).$$

The existence of $E^*(V^*, H^*, P^*, S^*, U^*)$. Where, V^*, H^*, P^*, S^* and U^* are the positive solutions of the algebraic equations given as

$$\begin{aligned} \eta - \psi_1 H^* - \eta_1 V^* - \psi_2 P^* V^* &= 0, \\ \gamma - \frac{\gamma}{L} H^* + \lambda\psi_1 H^* &= 0, \\ \mu H^* - \rho_0 P^* - \rho_1 S^* P^* &= 0, \\ \Delta - \pi_0 - \pi_1 V^* - \pi_2 P^* - \pi_3 P^{*2} &= 0, \\ \pi_1 V^* S^* - \phi_1 U^* - \phi_0 V^* U^* &= 0, \end{aligned} \tag{2}$$

Thus, from the second equation of the system (2), we have

$$\begin{aligned} H^* &= \frac{L}{\gamma} (\gamma + \lambda\psi_1 V^*), \quad V^* = \frac{\eta - \psi_1 H^*}{\eta_1 + \psi_2 P^*}, \quad P^* = \frac{\mu L (\gamma + \lambda\psi_1 V^*)}{\gamma(\rho_0 + \rho_1 S^*)}, \\ S^* &= \frac{\Delta}{\pi_0 + \pi_1 V^* + \pi_2 P^* + \pi_3 P^{*2}}, \quad U^* = \frac{\pi_0 S^* V^*}{\phi_0 + \phi_0 V^*}. \end{aligned} \tag{3}$$

Further, solving the equations in the system (3) in terms of P^* , we obtain

$$V^* = \frac{\gamma(\eta - \psi_1 L)}{\gamma\eta_1 + \lambda\psi_1^2 L + \gamma\psi_2 P^*} = f_1(P^*) \quad \text{and} \quad S^* = \frac{\Delta}{\pi_0 + \pi_1 f_1(P^*) + \pi_2 P^* + \pi_3 P^{*2}} = f_2(P^*) \text{ say.}$$

From which we further obtain

$$H^* = \frac{L}{\gamma} [\gamma + \lambda\psi_1 f_2(P^*)], \quad P^* = \frac{\mu L [\gamma + \lambda\psi_1 f_1(P^*)]}{\gamma[\rho_0 + \rho_1 f_2(P^*)]} \quad \text{and} \quad U^* = \frac{\pi_0 f_1(P^*) f_2(P^*)}{\phi_0 + \phi_0 f_1(P^*)}$$

It can therefore be gotten from the expression for P^* from the above that

$$\gamma P^* [\rho_0 + \rho_1 f_2(P^*)] = \mu L [\gamma + \lambda\psi_1 f_1(P^*)]$$

Thus, let

$$F(P^*) = \gamma P^* [\rho_0 + \rho_1 f_2(P^*)] - \mu L [\gamma + \lambda\psi_1 f_1(P^*)] = 0 \tag{4}$$

To establish the existence of E^* , it is sufficient to show that the equation (4) has unique positive solution P^* . We therefore proceed as follows.

1. $F(0) = -\mu L [\gamma + \lambda\psi_1 f_1(0)] < 0$ where $f_1(0) = \frac{\gamma(\eta - \psi_1 L)}{\gamma\eta_1 + \lambda\psi_1^2 L}$, provided $\eta > \psi_1 L$ as explained earlier.
2. $F\left(\frac{\mu L}{\rho_0}\right) = \gamma \mu L \left[\frac{\rho_0 \rho_1 a_1^2 \Delta - a_2 \rho_0 \psi_1 \lambda (\eta - \psi_1 L)}{a_1 a_2} \right] > 0$, given that $\rho_1 a_1^2 \Delta + a_2 \lambda \psi_1^2 L > \eta \lambda a_2 \psi_1$, where $a_1 = \gamma \rho_0 \eta_1 + \gamma \mu \psi_2 L + \lambda \rho_0 \psi_1^2 L > 0$ and $a_2 = \gamma \pi_1 \rho_0^3 (\eta - \psi_1 L) + a_1 [\pi_0 \rho_0^2 + \mu L (\rho_0 \pi_2 + \mu \pi_3 L)] > 0$.

Hence, there exists a P^* in the interval $0 < P^* < \mu L / \rho_0$ such that $F(P^*) = 0$.

To show the uniqueness of solution, we need to show that $\frac{dF(P^*)}{dt} < 0$.

$$3. \quad \frac{dF}{dt} = \gamma[\rho_0 + \rho_1 f_2(P^*)] + \gamma P^* \rho_2 \frac{df_1}{dt} - \mu L \lambda \psi_1 \frac{df_1}{dt}, \text{ where}$$

$$\frac{df_1}{dt} = -\frac{\gamma^2 \psi_2 (\eta - \psi_1 L)}{(\gamma \eta_1 + \lambda \psi_1^2 L + \gamma \psi_2 P^*)^2} \text{ and } \frac{df_2}{dt} = -\frac{\Delta[\pi_1 f_1(P^*) + \pi_2 + 2\pi_3 P^*]}{[\pi_0 + \pi_1 f_1(P^*) + \pi_2 P^* + \pi_3 P^{*2}]}$$

Thus, for the value P^* , the ensuing values of V^* , H^* , S^* and U^* can be obtained from the above. It can further noted that $\frac{dF}{d\mu} = -L[\gamma + \lambda \psi_1 f_1(P^*)] < 0$. Hence, the cumulative mass of fertile topsoil would decrease as the growth rate coefficient of population pressure increases. Similarly, $F(P^*) = \gamma P^* [\rho_0 + \rho_1 f_2(P^*)] - \mu L [\gamma + \lambda \psi_1 f_1(P^*)] = 0$

5. Stability analysis

5.1. Local stability analysis

Using the corresponding Jacobian matrix of the model system (1), the local stability behaviour of the equilibrium points $E_0, E_1, E_2, E_3, E_4, E_5, E_6, E_7, E_8, E_9$ and E_{10} may be analysed by determining the signs of the eigenvalues of the corresponding Jacobian matrix evaluated at point. Therefore, the Jacobian matrix of the model system (1) is

$$J = \begin{pmatrix} a_{11} & -\psi_1 V & -\psi_2 V^2 & 0 & 0 \\ \lambda \psi_1 H & \gamma \left(1 - \frac{2H}{L}\right) + \lambda \psi_1 V & 0 & 0 & 0 \\ 0 & \mu & -\rho_0 - \rho_1 S & -\rho_1 P & 0 \\ -\pi_1 S & 0 & -\pi_2 S - 2\pi_3 S P & -a_{44} & 0 \\ \pi_1 S & 0 & 0 & \pi_1 V & -\phi_1 - \phi_0 V \end{pmatrix},$$

where

$$a_{11} = \eta - \psi_1 H - 2(\eta_1 + \psi_2 P)V \text{ and } a_{44} = \pi_0 + \pi_1 V + \pi_2 P + \pi_3 P^2$$

Evaluating the Jacobian matrix at each equilibrium, we obtain the following results

1. Two of the eigenvalues of the Jacobian matrix J corresponding to the equilibrium E_0 are observed to be positive. So the equilibrium has unstable local manifold in the $V - H$ plane.
2. One of the eigenvalues of the Jacobian matrix J corresponding to the equilibrium E_1 is positive. So the equilibrium has an unstable local manifold in the H direction
3. The equilibrium E_2 is locally stable since all its eigenvalues are negative
4. It may be noted that two of the eigenvalues of J corresponding to E_3 are positive. So the equilibrium has an unstable local manifold in the $V - H$ plane.
5. The equilibrium E_4 is locally stable.
6. The matrix J corresponding to E_5 can be verified to have one positive eigenvalue. So the equilibrium has an unstable local manifold in the H direction.
7. Similarly with J having one positive eigenvalue when evaluated at E_6 , the equilibrium point has an unstable local manifold in the V direction.
8. Also one of the eigenvalues of J corresponding to equilibrium E_7 is positive. So the equilibrium has an unstable local manifold in the V plane.
9. The equilibrium point E_8 is locally stable.
10. Similarly, the equilibrium point E_9 is locally stable.

In view of the nature of the components of the interior equilibrium E^* , establishing its stability behaviour using the Jacobian scheme is quite rigorous and barely tractable. Thus, we state the following theorems which give sufficient conditions that guarantee its local and nonlinear stability.

Theorem 1. *The interior equilibrium E^* is locally asymptotically stable if the following conditions*

$$\left[\frac{2\gamma \rho_1 P^*}{3\mu^2 \lambda L} (\rho_0 + \rho_1 S^*) + \frac{\pi_2 S^* + 2\pi_3 S^* P^*}{\rho_0 + \rho_1 S^*} \right]^2 < \frac{8\gamma}{27\mu^2 \lambda L} (\rho_0 + \rho_1 S^*) (\pi_0 + \pi_1 V^* + \pi_2 P^* + \pi_3 P^{*2}) \tag{5}$$

and

$$\frac{\pi_1^2}{\eta_1 + \psi_2 P^*} < \min \left\{ \frac{2\gamma \pi_1^2 (\rho_0 + \rho_1 S^*)^2}{9\lambda \mu^2 \psi_2^2 L V^{*2}}, \frac{(\rho_0 + \rho_1 S^*) (\pi_0 + \pi_1 V^* + \pi_2 P^* + \pi_3 P^{*2})}{3S^{*2}}, \frac{(\eta_1 + \psi_2 P^*) (\phi_1 + \phi_0 V^*)}{2S^{*2}}, \frac{2(\phi_1 + \phi_0 V^*) (\pi_0 + \pi_1 V^* + \pi_2 P^* + \pi_3 P^{*2})}{3(\rho_0 + \rho_1 S^*) V^{*2}} \right\} \tag{6}$$

hold.

Proof

We employ the Lyapunov stability theorem to establish this claim. To achieve this, we consider the following positive definite function

$$L_1 = \frac{1}{2} \left(\frac{V_1^2}{V^*} + d_1 \frac{H_1^2}{H^*} + d_2 P_1^2 + d_3 S_1^2 + d_4 U_1^2 \right),$$

such that

$$V = V^* + V_1, \quad H = H^* + H_1, \quad P = P^* + P_1, \quad S = S^* + S_1, \quad U = U^* + U_1,$$

where V_1, H_1, P_1, S_1 and U_1 are small perturbations around the interior equilibrium E^* . Then the time derivative of L_1 along the solutions of the linearised system of the model system (1) is

$$\begin{aligned} \frac{dL_1}{dt} = & -(\eta_1 + \psi_2 P^*) V_1^2 - d_1 \frac{\gamma}{L} H_1^2 - d_2 (\rho_0 + \rho_1 S^*) P_1^2 - d_3 (\pi_0 + \pi_1 V^* + \pi_2 P^* + \pi_3 P^{*2}) S_1^2 \\ & - d_4 (\phi_1 + \phi_0 V^*) U_1^2 - \psi_2 V^* P_1 V_1 - \psi_1 (1 - d_1 \lambda) H_1 V_1 + d_2 \mu H_1 P_1 + d_4 \pi_1 S^* U_1 V_1 \\ & + d_4 \pi_1 V^* S_1 U_1 - d_3 \pi_1 S^* V_1 S_1 - [d_2 \rho_1 P^* + d_3 (\pi_2 S^* + 2\pi_3 S^* P^*)] P_1 S_1 \end{aligned} \tag{7}$$

Choosing

$$d_1 = \frac{1}{\lambda}, \quad d_3 = \frac{1}{\rho_0 + \rho_1 S^*} \quad \text{and} \quad d_4 = 1, \quad \text{then}$$

$$\begin{aligned} \psi_1^2 V^{*2} & < \frac{d_2}{3} (\eta_1 + \psi_2 P^*) (\rho_0 + \rho_1 S^*); \quad \pi_1^2 V^{*2} < \frac{2 (\phi_1 + \phi_0 V^*) (\pi_0 + \pi_1 V^* + \pi_2 P^* + \pi_3 P^{*2})}{\rho_0 + \rho_1 S^*}; \\ \pi_1^2 S^{*2} & < \frac{(\rho_0 + \rho_1 S^*) (\eta_1 + \psi_2 P^*) (\pi_0 + \pi_1 V^* + \pi_2 P^* + \pi_3 P^{*2})}{3}; \quad \pi_1^2 S^{*2} < \frac{1}{2} (\eta_1 + \psi_2 P^*) (\phi_1 + \phi_0 V^*); \end{aligned} \tag{8}$$

$$d_2 \mu^2 < \frac{2}{3} \frac{\gamma}{\lambda L} (\rho_0 + \rho_1 S^*); \quad \left[d_2 \rho_1 P^* + \frac{\pi_1 S^* + 2\pi_3 S^* P^*}{\rho_0 + \rho_1 S^*} \right]^2 < \frac{4}{9} d_2 (\pi_0 + \pi_1 V^* + \pi_2 P^* + \pi_3 P^{*2})$$

From inequalities (8), we may easily choose the positive value d_2 if

$$\frac{3\psi_2^2 V^{*2}}{(\eta_1 + \psi_2 P^*) (\rho_0 + \rho_1 S^*)} < d_2 < \frac{\gamma (\rho_0 + \rho_1 S^*)}{\lambda \mu^2 L}. \tag{9}$$

We assert from inequality (9) that $\frac{dL_1}{dt}$ is negative definite under condition (6) and (7), thus proving the claim.

5.2. Global stability analysis

To discuss the global stability behaviour of the interior equilibrium E^* , we state the following theorem.

Theorem 2. *The equilibrium E^* is globally asymptotically stable inside the region of attraction Ω , if the following conditions*

$$\left[\pi_2 + (\rho_1 m_2 + 2\pi_3) P^* \right]^2 < \frac{4m_2}{9S^*} (\rho_0 + \rho_1 S^*) (\pi_0 + \pi_1 V^* + \pi_2 P^* + \pi_3 P^{*2}) \tag{10}$$

and

$$\frac{3\pi_1^2 S^{*2}}{\eta_1 + \psi_2 P^*} < \min \left\{ \frac{1}{6}, \frac{2S^* (\pi_0 + \pi_1 V^* + \pi_2 P^* + \pi_3 P^{*2})}{(\eta_1 + \psi_2 P^*) V^{*2}}, S^* (\pi_0 + \pi_1 V^* + \pi_2 P^* + \pi_3 P^{*2}) \right\} \tag{11}$$

hold.

Proof

To establish the nonlinear stability behaviour of E^* , we consider the following positive definite function about E^*

$$L_2 = \left(V - V^* - V^* \ln \frac{V}{V^*} \right) + m_1 \left(H - H^* - H^* \ln \frac{H}{H^*} \right) + \frac{m_2}{2} (P - P^*)^2 + \frac{m_3}{2} (S - S^*)^2 + \frac{m_4}{2} (U - U^*),$$

where the constants m_1, m_2, m_3 and m_4 are positive and remain to be suitably chosen.

Evaluating the time derivative of L_2 along the solutions of the model system (1) for $m_1 = 1/\lambda, m_3 = 1/S^*$ and $m_4 = \phi_1 + \phi_0 V^*$, we obtain

$$\begin{aligned} L_2 = & -(\eta_1 + \psi_2 P^*) (V - V^*)^2 - m_1 \frac{\gamma}{L} (H - H^*)^2 - m_2 (\rho_0 + \rho_1 S^*) (P - P^*)^2 - m_4 (\phi_1 + \phi_0 V^*) (U - U^*)^2 \\ & - m_3 (\pi_0 + \pi_1 V^* + \pi_2 P^* + \pi_3 P^{*2}) (S - S^*)^2 + [m_2 \rho_1 P^* + m_3 (\pi_2 + 2\pi_3 P^*) S^*] (P - P^*) (S - S^*) \\ & - \psi_2 V^* (P - P^*) (V - V^*) + m_4 \pi_1 S^* (U - U^*) (V - V^*) + m_4 \pi_1 V^* (S - S^*) (U - U^*) - m_3 \pi_3 S^* (S - S^*) (V - V^*) \end{aligned}$$

Thus, $\frac{dL_2}{dt}$ will be negative definite inside the region of attraction Ω , provided the following inequalities

$$\psi_2^2 V^{*2} < \frac{m_2}{3} (\rho_0 + \rho_1 S^*) (\eta_1 + \psi_2 P^*),$$

$$m_2 \mu^2 < \frac{2}{3} \frac{\gamma}{\lambda L} (\rho_0 + \rho_1 S^*),$$

$$\pi_1^2 S^{*2} < \frac{1}{2} (\eta_1 + \psi_2 P^*),$$

$$[\pi_2 + (m_2 \rho_1 + 2\pi_3) P^*]^2 < \frac{4m_2}{9} (\rho_0 + \rho_1 S^*) (\pi_0 + \pi_1 V^* + \pi_2 P^* + \pi_3 P^{*2}),$$

$$\pi_1^2 V^{*2} < \frac{2}{3S^*} (\pi_0 + \pi_1 V^* + \pi_2 P^* + \pi_3 P^{*2}),$$

$$\pi_1^2 S^* < \frac{1}{3} (\eta_1 + \psi_2 P^*) (\pi_0 + \pi_1 V^* + \pi_2 P^* + \pi_3 P^{*2})$$

hold. It may easily be verified that the condition (11) is satisfied for our choice of parameter values (12). Furthermore, a set of positive suitable values of m_2 exist for which the inequality (10) is satisfied. More specifically, for instance, we may choose

$$m_2 = \frac{\gamma(\rho_0 + \rho_1 S^*)}{2\lambda\mu^2 L} = 2501.325$$

for such a verification. Thus, dL_2/dt is negative definite under conditions (10) and (11).

6. Numerical simulations

To investigate the feasibility of the results presented in the previous sections, we consider simulating our model numerically. Pursuant to this, we choose the following values for our parameters:

$$\eta = 0.8, \eta_1 = 0.065, \psi_1 = 0.002, \psi_2 = 0.0001, \gamma = 0.5, L = 100, \lambda = 0.05, \mu = 0.002, \rho_0 = 0.2, \quad (12)$$

$$\rho_1 = 0.005, \Delta = 0.95, \pi_0 = 0.5, \pi_1 = 0.805, \pi_2 = 0.95, \pi_3 = 0.008, \phi_0 = 0.8, \phi_1 = 0.005.$$

Thus, from the set of parameter values (12), we have obtained the components of the interior equilibrium E^* as $V^* = 10.0149, H^* = 888.2912, P^* = 16.1164, S^* = 0.0212, U^* = 0.0206$.

Further, the corresponding eigenvalues of the Jacobian matrix around E^* of the model system (1) are given as: -0.7108, -0.38191, -0.2001, -44.6516, -8.0169. The negative signs of all the corresponding eigenvalues validate the local stability of the interior equilibrium E^* with respect to the set of parameter values (12). Its global stability, on the other hand, has been shown in figure (1). It may be understood from these figures that each sub-density attains its stability, thus, confirming the stability of the interior equilibrium. Furthermore, the extent of the baseline parameters on the dynamics of the model system reveals the following: it is shown in figure 2 that increasing η_1 (that is, the depletion rate of vegetation cover due to human intraspecific competition), the mass of fertile topsoil and the density of vegetation cover with respect to time would increase the mass of fertile topsoil but decrease the density of vegetation cover. A similar scenario is observed in figures 3 and 4 as ψ_1 and ψ_2 are increased respectively. That is, the figures show that increasing demand on vegetation resource for herbs, firewood, fodder, roofing, shelter and wood as well as those needs bordering on expansion for agriculture and infrastructure would lead to decreasing the density of vegetation and as a result increase in the mass of fertile topsoil. It can be observed from figure 5 that the equilibrium levels of $S(t)$ and $V(t)$ simultaneously decrease with increasing values of μ , that is, as the growth rate coefficient of population pressure due to population increases. The effect of the declination of population pressure due to natural and deployment factors is shown in figures 6 and 7.

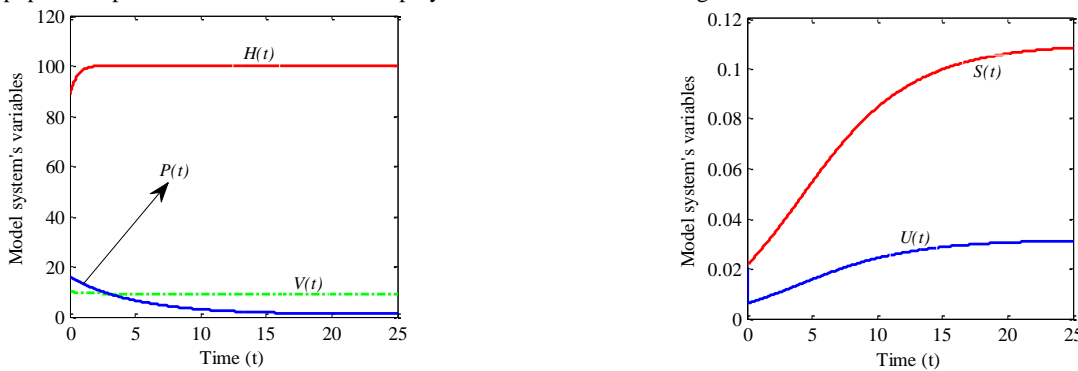


Figure 1. Density of model's variables $V(t), H(t), P(t), S(t)$ and $U(t)$ at the interior equilibrium, E^* , against time t for parameter values in (12).

Form these figures, we observe that as the values of ρ_0 and ρ_1 increase, the equilibrium levels of fertile topsoil and vegetation cover decrease.



Figure 2. Variation of $S(t)$ and $V(t)$ against time t for various values of η_1 while values of other parameters are held as in equation (12).



Figure 3. Variation of $S(t)$ and $V(t)$ against time t for various values of ψ_1 while values of other parameters are held as in equation (12).

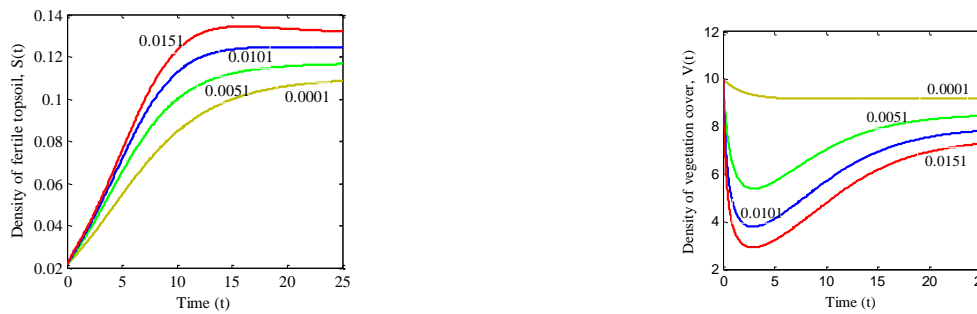


Figure 4. Variation of $S(t)$ and $V(t)$ against time t for various values of ψ_2 while values of other parameters are held as in equation (12).



Figure 5. Variation of $S(t)$ and $V(t)$ against time t for various values of μ while values of other parameters are held as in equation (12).



Figure 6. Variation of $S(t)$ and $V(t)$ against time t for various values of ρ_0 while values of other parameters are held as in equation (12).

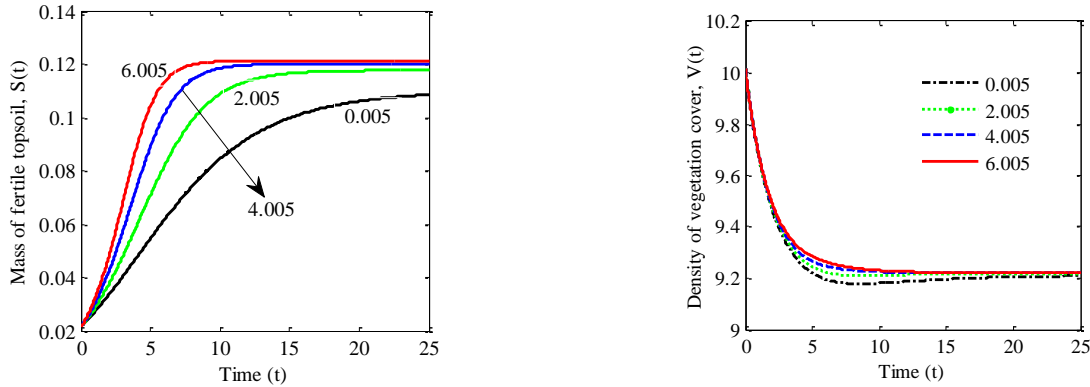


Figure 7. Variation of $S(t)$ against time t for various values of ρ_1 while values of other parameters are held as in equation (12).

7. Conclusion

Increase in human population is exerting enormous pressures on the ecosystem that resulting in phenomenal system imbalances. Topsoil fertility alongside free existing natural resources which dependant on it are being affected at depletive levels. To investigate the consequential fallout of this problem, a nonlinear mathematical model has been developed. In this model, we have considered a logistic growth for both the human population and vegetation cover. The density of fertile topsoil is considered to be simultaneously pressured by growing human population and vegetation cover both needing sustenance. We analysed the model using the stability theory of differential equations. All the 11 feasible equilibria of the model were analysed for both local and global asymptotic stability. In addition, numerical simulations were performed to validate the analytical results. In particular, it was found that deploying increasing volumes of human pressure could deplete both fertile topsoil and vegetation cover.

References

- [1] E. Sebastian and P. Victor (2017). Modelling Deforestation due to Human Population and its effect on Farm Fields. *Journal of Informatics and Mathematical Sciences* **9** 903 – 913.
- [2] Michel De Lara and Luc Doyen (2008). *Sustainable Management of Natural Resources. Mathematical Models and Methods*. Springer. ISBN:978-3-540-79073-0.
- [3] G. Wall - Ontario Institute of Pedology; C.S. Baldwin – Ridgetown College of Agricultural Technology; I.J. Shelton - Ontario Institute of Pedology.
- [4] G.C. Sander, T. Zheng, P. Heng, Y. Zhong and D.A. Barry (2011). Sustainable soil and water resources: modelling soil erosion and its impact on the environment 19th International Congress on Modelling and Simulation, Perth, Australia, 12–16 December 2011 <http://mssanz.org.au/modsim2011>.
- [5] Y. P. Li, G. H. Huang, S. L. Nie, B. Chen, and X. S. Qin (2013). *Mathematical Modeling for Resources and Environmental Systems. Mathematical Problems in Engineering*. <http://dx.doi.org/10.1155/2013/674316>
- [6] K. Misra, K. Lata, J. B. Shukla (2013). Effects of population and population pressure on forest resources and their conservation: A Modeling study. *Environ Dev Sustain*. DOI: 10.1007/s10668-013-9481-x.
- [7] K. Lata, A.K. Misra, J.B. Shukla (2018). Modeling the effect of deforestation caused by human population pressure on wildlife species. *Nonlinear Analysis: Modelling and Control*, **23**(4) No. 3, 303–320. <https://doi.org/10.15388/NA.2018.3.2>
- [8] Vivi Ramdhani (2015). Dynamical System of Modelling the Depletion of Forestry Resources Due to Crowding by Industrialization. *Applied Mathematical Sciences*, **9**, 4067 – 4079 <http://dx.doi.org/10.12988/ams.2015.53259>.
- [9] K. Lata, A.K. Misra (2017). Modeling the effect of economic efforts to control population pressure and conserve forestry resources. *Nonlinear Analysis: Modelling and Control*, **22**(4) 473 – 488.
- [10] J.B. Shukla (2011). Modeling the Depletion of a Renewable Resource by Population and Industrialization: Effect of Technology on its Conservation. *Natural Resource Modeling*, **24**(2) 242 – 267.